JACS
JOURNAL OF THE AMERICAN CHEMICAL SOCIETY

Communication

pubs.acs.org/JACS

Reshaping Lithium Plating/Stripping Behavior via Bifunctional Polymer Electrolyte for Room-Temperature Solid Li Metal Batteries

Xian-Xiang Zeng,[†,‡] Ya-Xia Yin,[†,‡] Nian-Wu Li,[†] Wen-Cheng Du,[†,‡] Yu-Guo Guo,*[,†,‡] and Li-Jun Wan[†,‡]

[†]CAS Key Laboratory of Molecular Nanostructure and Nanotechnology, Institute of Chemistry, Chinese Academy of Sciences (CAS), Beijing 100190, P. R. China

[‡]School of Chemistry and Chemical Engineering, University of Chinese Academy of Sciences, Beijing 100049, P. R. China

Supporting Information

ABSTRACT: High-energy rechargeable Li metal batteries are hindered by dendrite growth due to the use of a liquid electrolyte. Solid polymer electrolytes, as promising candidates to solve the above issue, are expected to own high Li ion conductivity without sacrificing mechanical strength, which is still a big challenge to realize. In this study, a bifunctional solid polymer electrolyte exactly having these two merits is proposed with an interpenetrating network of poly(ether−acrylate) (ipn-PEA) and realized via photopolymerization of ion-conductive poly(ethylene oxide) and branched acrylate. The ipn-PEA electrolyte with facile processing capability integrates high mechanical strength (ca. 12 GPa) with high room-temperature ionic conductance (0.22 mS cm^{-1}), and significantly promotes uniform Li plating/stripping. Li metal full cells assembled with ipn-PEA electrolyte and cathodes within 4.5 V vs Li^+/Li operate effectively at a rate of 5 C and cycle stably at a rate of 1 C at room temperature. Because of its fabrication simplicity and compelling characteristics, the bifunctional ipn-PEA electrolyte reshapes the feasibility of room-temperature solid-state Li metal batteries.

The increasing demand for energy has facilitated the development of sustainable storage technologies,[1] and the high theoretical specific capacity of Li metal (3860 mA h g^{-1}) has revived the use of rechargeable batteries with Li metal as the anode in recent years.[2] However, the formation of dendritic Li during Li plating[3] hinders the development of Li-metal-based high-energy storage systems.[4] Advancements have been made to restrain dendrite formation and reinforce protection for the Li anode, including electrolytes,[5] electrodes,[6] separators,[7] and current collectors.[8] Unfortunately, Li is thermodynamically unstable with liquid electrolytes.[9] During the process of Li plating/stripping, the formed solid electrolyte interphase (SEI) usually cracks as a result of volumetric expansion, thereby leading to undesired dendrite growth and exposing fresh Li for further side reactions.

Solid-state Li secondary batteries are regarded as an ultimate solution to the aforementioned issues because of their perceived capability to mitigate and block the growth of dendrite nucleation[10] and allow assembly of cells in various package styles.[11] To achieve these goals, the solid electrolyte must have high ionic conductivity,[12] suitable mechanical strength,[13] and favorable electrochemical stability.[14] In view of the synthesis and processing difficulties in inorganic solid electrolytes,[15] solid polymer electrolytes are more efficient and feasible.[16] Nevertheless, issues such as the contradiction between high ionic conductivity and high mechanical strength[13c] and the narrow electrochemical stability window of nitrile- and ether-based electrolytes (4 V vs Li^+/Li)[17] hinder the applications of solid polymer electrolytes in high-energy solid-state Li batteries.

In this study, a novel solid-state polymer electrolyte with an interpenetrating poly(ether−acrylate) (ipn-PEA) network was developed via photopolymerization of ion-conductive poly(ethylene oxide) (PEO) and branched acrylate to obtain a rigid−flexible structure (Figure 1). The key is to integrate high

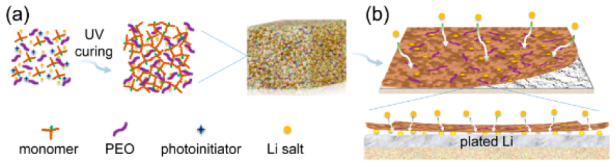

Figure 1. (a) Illustration of the preparation of the ipn-PEA electrolyte. (b) Proposed electrochemical deposition behavior of Li metal with ipn-PEA electrolyte.

Li ion conductivity with high mechanical strength in one solid-state electrolyte that reconciles the rigidity−conductivity inconsistency and satisfies the requirements for high-voltage cathodes and easy processability. The size-adjustable ipn-PEA electrolyte reveals a bifunctionality of high ion conductivity (0.22 mS cm^{-1}) at room temperature and high mechanical strength (ca. 12 GPa) as a result of the ideal combination of plasticity and rigidity, respectively, inherited from PEO and PEA. When paired with cathodes with a working potential within 4.5 V vs Li^+/Li, the ipn-PEA electrolyte enables a powerful cell that effectively operates at a rate of 5 C and delivers admirable specific capacity and cycling stability at a rate of 1 C at room temperature. More importantly, the ipn-PEA electrolyte formed in situ shows a conspicuous effect on blocking Li dendrite growth. On the basis of its facile synthesis

Received: September 26, 2016
Published: November 30, 2016

DOI: 10.1021/jacs.6b10088
J. Am. Chem. Soc. 2016, 138, 15825−15828

and excellent performance, the ipn-PEA electrolyte is a good reference for designing solid-state electrolytes and advancing the applications of other solid-state electrochemical energy storage systems.

The ipn-PEA electrolyte is obtained by photopolymerization of ethoxylated trimethylolpropane triacrylate in the existence of $LiPF_6$ and PEO (for synthesis details, see the Supporting Information). Taking Φ = 12 mm and Φ = 40 mm as examples, the ipn-PEA electrolyte exhibits outstanding flexibility and freely adjustable size (Figure 2a,b). The thickness of the ipn-PEA electrolyte is approximately 35 μm with a smooth surface and without phase separation (Figure 2c,d). The X-ray diffraction (XRD) pattern of pure PEO consists of two intense peaks (2θ = 19° and 23°) (Figure 2e), corresponding to the essential characteristics of the crystalline PEO. After polymerization, these crystalline peaks disappear, implying the amorphous phase of PEO, which was further verified by the Fourier transform infrared spectra (Figure S1). The reason could be that the branched acrylate forms interconnected "cages" that spatially besiege the PEO molecules and restrain PEO crystallization effectively.[18]

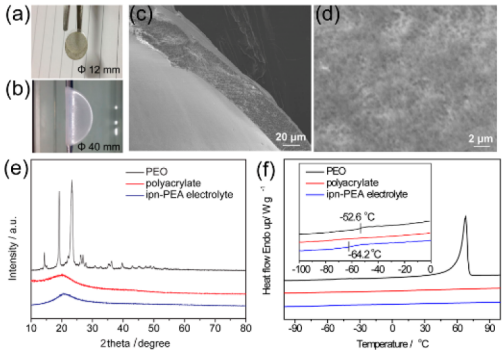

Figure 2. Photographs of ipn-PEA electrolytes with diameters of (a) 12 and (b) 40 mm. (c) Cross-ection and (d) top-view SEM images of the ipn-PEA electrolyte. (e) XRD spectra and (f) DSC curves of PEO, polyacrylate, and the ipn-PEA electrolyte.

The designed ipn-PEA electrolyte possesses an amorphous structure with a low glass transition temperature (T_g), which is evidenced by the lack of a melting-point peak in differential scanning calorimetry (DSC) curves over the temperature range from −100 to 100 °C (Figure 2f). The T_g of approximately −52.6 °C for pure PEO shifts negatively to approximately −64.2 °C in the ipn-PEA electrolyte. Meanwhile, no phase separation is observed by atomic force microscopy (Figure S2). This result portends the possession of fine chain mobility and low activation energy (E_a) for ion transport in the ipn-PEA electrolyte.[18b]

The Li-ion transference number (t_{Li}^+) of the ipn-PEA electrolyte is approximately 0.65 (Figure S3a), which overmatches those of common liquid electrolytes (t_{Li}^+ = 0.2−0.5).[19] The high t_{Li}^+ is efficient in preventing the formation of a large electric field within the space-charge region by immobilizing anions.[20] The room-temperature ionic conductivity (σ) attains 2.20×10^{-4} S cm^{-1} (Figure S3b). Moreover, σ increases with temperature (T) elevation and presents a temperature dependence, with the linear shape of the plot exhibiting a typical Arrhenius-type behavior with an E_a of approximately 0.39 eV (Figure S3c). All of the above results imply that no distinct structure change occurs in the ipn-PEA electrolyte within the testing temperature range and are beneficial for Li deposition and the rate capability of the battery.

The long-time cycling stability verifies the interfacial stability between the ipn-PEA electrolyte and Li metal (Figure S3d−f). The Li deposition behaviors with the ipn-PEA and liquid electrolytes are vastly different (Figure S4). Compared with the scanning electron microscopy (SEM) images of deposited Li in the liquid electrolyte (Figure 3a−d), the overall morphology of Li is smoother in the ipn-PEA electrolyte-modified Li foil[21] (Figure 3e−h) (see Figure S3 in the Supporting Information for details of Li depositon in the liquid and ipn-PEA electrolytes). On the basis of the Young's modulus (ca. 12 GPa)[22] (Figure 3i), we speculatively propose the illustration of Li deposition in liquid and ipn-PEA electrolytes shown in Figure 3j.

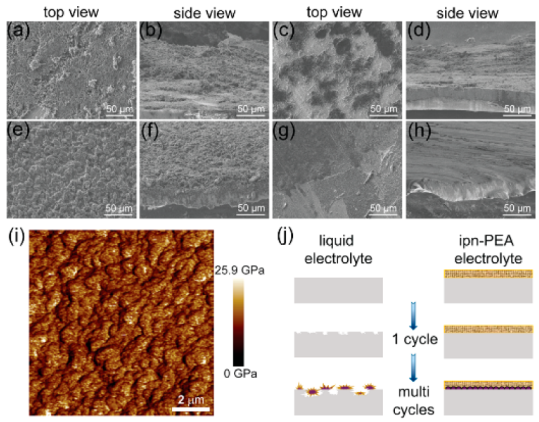

Figure 3. (a−h) SEM images of Li plating and stripping on Cu foil with liquid and ipn-PEA electrolytes for 2 mA h cm^{-2} at 0.5 mA cm^{-2}. Panels (a−d) and (e−h) are for the liquid and ipn-PEA electrolytes, respectively. Panels (a, b, e, f) and (c, d, g, h) are SEM images of Li plating and Li stripping, respectively. (i) Young's modulus mapping of the ipn-PEA electrolyte. (j) Illustration of the proposed Li deposition behavior using liquid and ipn-PEA electrolytes.

The ipn-PEA electrolyte is stable within 4.5 V vs Li^+/Li (Figure S5) with low electronic conductivity (1.56×10^{-8} S cm^{-1}) (Figure S6) and shows good thermal stability (Figure S7). Besides, the ipn-PEA electrolyte can be used to assemble batteries with close contact without a separator (Figure S8), which was verified by the energy-dispersive X-ray spectra (Figure S9) and cyclic voltammogram (Figure S10) of the $LiFePO_4$ (LFP) cathode.

The specific capacities of cells using the ipn-PEA electrolyte were approximately 141 and 66 mA h g^{-1} at 0.5 and 5 C, respectively (Figure 4a,b). After 200 cycling tests at 1 C, the capacity remained at nearly 85% of its initial capacity (Figure 4c). A solid-state battery with the ipn-PEA electrolyte working at such a high rate (5 C) is rare. The ipn-PEA electrolyte exhibited no morphology change or mechanical failure after 200 cycles (Figure S11), and the overpotential increased by only 0.18 V (Figure S12), which supports its excellent stability. The ipn-PEA electrolyte also satisfies safety and flexibility requirements, and no short circuit appears even after the pouch cell is cut (Figure 4d). Moreover, the pouch cell maintains the capability of lighting the LED device before (Figure 4e) and after bending tests (Figure 4f). In addition, the ipn-PEA electrolyte can be used in other cathodes with high working potential, such as $LiNi_{0.5}Co_{0.2}Mn_{0.3}O_2$ (Figure S13). The ipn-

DOI: 10.1021/jacs.6b10088
J. Am. Chem. Soc. 2016, 138, 15825−15828

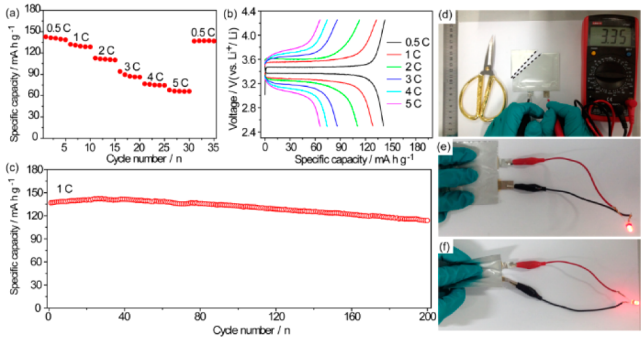

Figure 4. (a) Rate capabilities and (b) corresponding galvanostatic discharge/charge voltage profiles for a Lilipn-PEA electrolyte|LFP battery. (c) Cycling performances for the solid battery at a rate of 1 C. All of the above tests were conducted at room temperature (25 °C). (d) Photograph showing the voltage of a Lilipn-PEA electrolyte|LFP pouch cell after being cut. The LED device can be lighted before (e) and after (f) the bending test.

PEA structure is compatible with other Li salts (Figure S14). The effects of the ipn-PEA electrolyte on the Li plating/stripping behavior were characterized by SEM (Figure S15) and X-ray photoelectron spectroscopy (Figure S16). These results together with Table S1 indicate that the ipn-PEA electrolyte is satisfactory and favorable for reducing side reactions, sustaining a stable SEI, and obtaining uniform Li plating/stripping during cycling.

In conclusion, a novel rigid−flexible structure of polymer electrolytes is proposed and demonstrated by the ipn-PEA electrolyte for room-temperature solid-state Li metal batteries. The remarkable characteristics of the ipn-PEA electrolyte are attributed to the following aspects: the ductile PEO softens the rigid PEA network to ameliorate the contact between the electrodes and electrolyte and reduce the interfacial resistance; the interconnected "cages" in the PEA network spatially besiege the PEO and inhibit PEO crystallization to guarantee fast transport of Li^+; and the Li dendrite is blocked by pressure exerted from the rigid PEA network. Consequently, the ipn-PEA electrolyte formed on the Li surface realizes the dual function of suppressed dendrite growth for stable battery cycling and enhanced kinetics for high-rate operation of the battery. The ipn-PEA electrolyte developed in this study reshapes the feasibility of room-temperature solid-state Li metal batteries and will further advance the comprehension of interface compatibility between the constituents and structural features in the design of other solid-state electrochemical energy storage systems.

■ ASSOCIATED CONTENT

Supporting Information

The Supporting Information is available free of charge on the ACS Publications website at DOI: 10.1021/jacs.6b10088.

Experimental details and additional data (PDF)

■ AUTHOR INFORMATION

Corresponding Author

*ygguo@iccas.ac.cn

ORCID

Yu-Guo Guo: 0000-0003-0322-8476

Li-Jun Wan: 0000-0002-0656-0936

Notes

The authors declare no competing financial interest.

■ ACKNOWLEDGMENTS

This work was supported by the Ministry of Science and Technology of the People's Republic of China (Grant 2016YFA0202500), the National Natural Science Foundation of China (Grants 51225204, U1301244, and 21127901), the "Strategic Priority Research Program" of the Chinese Academy of Sciences (Grant XDA09010300), and the Chinese Academy of Sciences. The authors thank Dr. Sen Xin for helpful discussions.

■ REFERENCES

(1) (a) Tarascon, J. M.; Armand, M. *Nature* **2001**, *414*, 359. (b) Goodenough, J. B.; Park, K. S. *J. Am. Chem. Soc.* **2013**, *135*, 1167. (c) Zu, C.-X.; Li, H. *Energy Environ. Sci.* **2011**, *4*, 2614.

(2) (a) Bruce, P. G.; Freunberger, S. A.; Hardwick, L. J.; Tarascon, J.-M. *Nat. Mater.* **2012**, *11*, 19. (b) Yin, Y. X.; Xin, S.; Guo, Y. G.; Wan, L. J. *Angew. Chem., Int. Ed.* **2013**, *52*, 13186. (c) Kim, H.; Jeong, G.; Kim, Y.-U.; Kim, J.-H.; Park, C.-M.; Sohn, H.-J. *Chem. Soc. Rev.* **2013**, *42*, 9011.

(3) (a) Bhattacharyya, R.; Key, B.; Chen, H.; Best, A. S.; Hollenkamp, A. F.; Grey, C. P. *Nat. Mater.* **2010**, *9*, 504. (b) Harry, K. J.; Hallinan, D. T.; Parkinson, D. Y.; MacDowell, A. A.; Balsara, N. P. *Nat. Mater.* **2014**, *13*, 69.

(4) (a) Xu, W.; Wang, J.; Ding, F.; Chen, X.; Nasybulin, E.; Zhang, Y.; Zhang, J.-G. *Energy Environ. Sci.* **2014**, *7*, 513. (b) Choi, J. W.; Aurbach, D. *Nat. Rev. Mater.* **2016**, *1*, 16013.

(5) (a) Ding, F.; Xu, W.; Graff, G. L.; Zhang, J.; Sushko, M. L.; Chen, X.; Shao, Y.; Engelhard, M. H.; Nie, Z.; Xiao, J.; Liu, X.; Sushko, P. V.; Liu, J.; Zhang, J.-G. *J. Am. Chem. Soc.* **2013**, *135*, 4450. (b) Lu, Y.; Tu, Z.; Archer, L. A. *Nat. Mater.* **2014**, *13*, 961. (c) Wang, J.; Yamada, Y.; Sodeyama, K.; Chiang, C. H.; Tateyama, Y.; Yamada, A. *Nat. Commun.* **2016**, *7*, 12032.

(6) (a) Kozen, A. C.; Lin, C. F.; Pearse, A. J.; Schroeder, M. A.; Han, X.; Hu, L.; Lee, S. B.; Rubloff, G. W.; Noked, M. *ACS Nano* **2015**, *9*, 5884. (b) Ryou, M.-H.; Lee, Y. M.; Lee, Y.; Winter, M.; Bieker, P. *Adv. Funct. Mater.* **2015**, *25*, 834. (c) Cheng, X.-B.; Hou, T.-Z.; Zhang, R.; Peng, H.-J.; Zhao, C.-Z.; Huang, J.-Q.; Zhang, Q. *Adv. Mater.* **2016**, *28*, 2888. (d) Zheng, G.; Lee, S. W.; Liang, Z.; Lee, H. W.; Yan, K.; Yao, H.; Wang, H.; Li, W.; Chu, S.; Cui, Y. *Nat. Nanotechnol.* **2014**, *9*, 618.

(7) (a) Luo, W.; Zhou, L.; Fu, K.; Yang, Z.; Wan, J.; Manno, M.; Yao, Y.; Zhu, H.; Yang, B.; Hu, L. *Nano Lett.* **2015**, *15*, 6149. (b) Tung, S. O.; Ho, S.; Yang, M.; Zhang, R.; Kotov, N. A. *Nat. Commun.* **2015**, *6*, 6152.

(8) (a) Yang, C. P.; Yin, Y. X.; Zhang, S. F.; Li, N. W.; Guo, Y. G. *Nat. Commun.* **2015**, *6*, 8058. (b) Chen, Z.; Hsu, P.-C.; Lopez, J.; Li, Y.; To, J. W. F.; Liu, N.; Wang, C.; Andrews, S C.; Liu, J.; Cui, Y.; Bao, Z. *Nat. Energy* **2016**, *1*, 15009.

(9) Aurbach, D.; Zinigrad, E.; Cohen, Y.; Teller, H. *Solid State Ionics* **2002**, *148*, 405.

(10) (a) Kamaya, N.; Homma, K.; Yamakawa, Y.; Hirayama, M.; Kanno, R.; Yonemura, M.; Kamiyama, T.; Kato, Y.; Hama, S.; Kawamoto, K.; Mitsui, A. *Nat. Mater.* **2011**, *10*, 682. (b) Bouchet, R.; Maria, S.; Meziane, R.; Aboulaich, A.; Lienafa, L.; Bonnet, J.-P.; Phan, T. N. T.; Bertin, D.; Gigmes, D.; Devaux, D.; Denoyel, R.; Armand, M. *Nat. Mater.* **2013**, *12*, 452.

(11) (a) Li, J.; Ma, C.; Chi, M.; Liang, C.; Dudney, N. J. *Adv. Energy Mater.* **2015**, *5*, 1401408. (b) Robinson, A. L.; Janek, J. *MRS Bull.* **2014**, *39*, 1046.

(12) (a) Seino, Y.; Ota, T.; Takada, K.; Hayashi, A.; Tatsumisago, M. *Energy Environ. Sci.* **2014**, *7*, 627. (b) Kato, Y.; Hori, S.; Saito, T.; Suzuki, K.; Hirayama, M.; Mitsui, A.; Yonemura, M.; Iba, H.; Kanno, R. *Nat. Energy* **2016**, *1*, 16030.

(13) (a) Zhang, J.; Zhao, J.; Yue, L.; Wang, Q.; Chai, J.; Liu, Z.; Zhou, X.; Li, H.; Guo, Y.; Cui, G.; Chen, L. *Adv. Energy Mater.* **2015**, *5*,

DOI: 10.1021/jacs.6b10088
J. Am. Chem. Soc. 2016, 138, 15825−15828

1501082. (b) Zhou, D.; Liu, R.; He, Y.-B.; Li, F.; Liu, M.; Li, B.; Yang, Q.-H.; Cai, Q.; Kang, F. *Adv. Energy Mater.* **2016**, *6*, 1502214. (c) Zhou, W.; Wang, S.; Li, Y.; Xin, S.; Manthiram, A.; Goodenough, J. B. *J. Am. Chem. Soc.* **2016**, *138*, 9385.
(14) Rangasamy, E.; Liu, Z.; Gobet, M.; Pilar, K.; Sahu, G.; Zhou, W.; Wu, H.; Greenbaum, S.; Liang, C. *J. Am. Chem. Soc.* **2015**, *137*, 1384.
(15) Park, K. H.; Oh, D. Y.; Choi, Y. E.; Nam, Y. J.; Han, L.; Kim, J. Y.; Xin, H.; Lin, F.; Oh, S. M.; Jung, Y. S. *Adv. Mater.* **2016**, *28*, 1874.
(16) (a) Aetukuri, N. B.; Kitajima, S.; Jung, E.; Thompson, L. E.; Virwani, K.; Reich, M.-L.; Kunze, M.; Schneider, M.; Schmidbauer, W.; Wilcke, W. W.; Bethune, D. S.; Scott, J. C.; Miller, R. D.; Kim, H.-C. *Adv. Energy Mater.* **2015**, *5*, 1500265. (b) Kil, E.-H.; Choi, K.-H.; Ha, H.-J.; Xu, S.; Rogers, J. A.; Kim, M. R.; Lee, Y.-G.; Kim, K. M.; Cho, K. Y.; Lee, S.-Y. *Adv. Mater.* **2013**, *25*, 1395. (c) Pan, Q.; Smith, D. M.; Qi, H.; Wang, S.; Li, C. Y. *Adv. Mater.* **2015**, *27*, 5995. (d) Zhu, Z.; Hong, M.; Guo, D.; Shi, J.; Tao, Z.; Chen, J. *J. Am. Chem. Soc.* **2014**, *136*, 16461.
(17) (a) Guyomard, D.; Tarascon, J. M. *J. Electrochem. Soc.* **1993**, *140*, 3071. (b) Wetjen, M.; Kim, G.-T.; Joost, M.; Appetecchi, G. B.; Winter, M.; Passerini, S. *J. Power Sources* **2014**, *246*, 846. (c) Zaghib, K.; Armand, M.; Gauthier, M. *J. Electrochem. Soc.* **1998**, *145*, 3135. (d) Seki, S.; Kobayashi, Y.; Miyashiro, H.; Mita, Y.; Iwahori, T. *Chem. Mater.* **2005**, *17*, 2041. (e) Li, Q.; Imanishi, N.; Hirano, A.; Takeda, Y.; Yamamoto, O. *J. Power Sources* **2002**, *110*, 38. (f) Matoba, Y.; Matsui, S.; Tabuchi, M.; Sakai, T. *J. Power Sources* **2004**, *137*, 284.
(18) (a) Liu, G.; Reinhout, M.; Mainguy, B.; Baker, G. L. *Macromolecules* **2006**, *39*, 4726. (b) Croce, F.; Appetecchi, G. B.; Persi, L.; Scrosati, B. *Nature* **1998**, *394*, 456.
(19) (a) Xu, K. *Chem. Rev.* **2014**, *114*, 11503. (b) Bachman, J. C.; Muy, S.; Grimaud, A.; Chang, H.-H.; Pour, N.; Lux, S. F.; Paschos, O.; Maglia, F.; Lupart, S.; Lamp, P.; Giordano, L.; Yang, S.-H. *Chem. Rev.* **2016**, *116*, 140.
(20) (a) Chazalviel, J. N. *Phys. Rev. A* **1990**, *42*, 7355. (b) Ma, Q.; Zhang, H.; Zhou, C.; Zheng, L.; Cheng, P.; Nie, J.; Feng, W.; Hu, Y.-S.; Li, H.; Huang, X.; Chen, L.; Armand, M.; Zhou, Z. *Angew. Chem., Int. Ed.* **2016**, *55*, 2521.
(21) (a) Qian, J.; Henderson, W. A.; Xu, W.; Bhattacharya, P.; Engelhard, M.; Borodin, O.; Zhang, J.-G. *Nat. Commun.* **2015**, *6*, 6362. (b) Li, N. W.; Yin, Y. X.; Yang, C. P.; Guo, Y. G. *Adv. Mater.* **2016**, *28*, 1853.
(22) (a) Khurana, R.; Schaefer, J. L.; Archer, L. A.; Coates, G. W. *J. Am. Chem. Soc.* **2014**, *136*, 7395. (b) Monroe, C.; Newman, J. *J. Electrochem. Soc.* **2003**, *150*, A1377. (c) Stone, G. M.; Mullin, S. A.; Teran, A. A.; Hallinan, D. T.; Minor, A. M.; Hexemer, A.; Balsara, N. P. *J. Electrochem. Soc.* **2012**, *159*, A222.

DOI: 10.1021/jacs.6b10088
J. Am. Chem. Soc. 2016, 138, 15825−15828